RSC Advances

ROYAL SOCIETY OF CHEMISTRY

www.rsc.org/advances

New Nanoplatforms Based on Upconversion Nanoparticle and Single-Walled Carbon Nanohorns for Sensitive Detection of Acute Promyelocytic Leukemia

Yanxia Xu[a], Xianfu Meng[a], Jinliang Liu[a]*, Shuyun, Zhu[b]*, Lining Sun[a] and Liyi Shi[a]*

[a] Research Center of Nano Science and Technology, Shanghai University, Shanghai, 200444, China.

[b] Shandong Provincial Key Laboratory of Life-Organic Analysis, College of Chemistry and Chemical Engineering, Qufu Normal University, Qufu, Shandong, 273165, China.

*To whom correspondence should be addressed:

Dr. Jinliang Liu

Research Center of Nano Science and Technology, Shanghai University, 200444, China.

Phone: +86-21-66137197

Fax: +86-21-66137197

Email: liujl@shu.edu.cn

Dr. Shuyun Zhu

Shandong Provincial Key Laboratory of Life-Organic Analysis, College of Chemistry and Chemical Engineering, Qufu Normal University, Qufu, Shandong, 273165, China.

Email: shuyunzhu1981@163.com

Prof. Liyi Shi

Research Center of Nano Science and Technology, Shanghai University, 200444, China.

Phone: +86-21-66137208

Email: shiliyi@shu.edu.cn.

Abstract

A new luminescence "Turn-On" nanoplatform based on luminescence resonance energy transfer (LRET) from sodium citrate functionalized upconversion nanoparticles (Cit-UCNPs, energy donor) to single-walled carbon nanohorns (SWCNHs, energy acceptor) was prepared for sensitive detection of acute promyelocytic leukemia (APL). In the presence of the target DNA, a PML/RARα fusion gene of APL, the π-π stacking interaction between energy donor Cit-UCNPs and energy acceptor SWCNHs weakened and the their distance enlarged. Therefore, the luminescence of Cit-UCNPs would be recovered (turn on) due to the inhibition of the LRET process. Based on this fact, a sensitive method was developed for the fluorescent turn on detection of ALP with a detection limit as low as 0.28 nM. To the best of our knowledge, this is the first time that upconversion nanoparticles and single-walled carbon nanohorns were used as a donor-acceptor pair to detect PML/RARα fusion gene sequences through a LRET process.

Keywords: Upconversion nanoparticles; LRET; SWCNHs; APL

1. Introduction

Acute promyelocytic leukemia (APL) is a special leukemia accounting for above 10% adult acute myeloid leukemia.[1, 2] APL can lead the proliferation of leukemia cells and inhibit the generation of normal blood cells.[3] People suffering from APL often go with bleeding severely and the bleeding mechanism is very complex.[4-7] The t(15;17) (q22;q21) is a specific chromosome reciprocal translocation of APL, resulting in the generation of fusion gene between retinoic acid receptor alpha (RARα) and promyelocytic leukemia (PML) at the molecular level.[8] The formation of PML/RARα fusion gene encodes the PML/RARα fusion protein, which blocks the differentiation and maturation of myeloid, resulting in cell cancerous.[9] Many research demonstrate that PML/RARα fusion gene can be regarded as the molecular biology pathogenesis of APL.[10,11] Recently, the most reported clinical diagnosis methods of PML/RARα fusion gene are flow cytometry (FCM),[12] chromosome analysis,[13] fluorescence in situ hybridization (FISH),[14,15] and real-time quantitative reverse transcription PCR (RT-PCR).[16] These methods often suffer from some disadvantages such as time-consuming, expensive equipment and unsuitable for performing assays in a general case.[17] Fluorometric assays based on luminescence resonance energy transfer (LRET) mechanism have been considered as a promising candidate for DNA detection, but the commonly used fluorescent materials such as semiconductor quantum dots and organic fluorescent dyes often suffer from some drawbacks, such as low chemical stability and hydrophobic property.[18] What's more, most of the reported LRET probes showed a ''turn-off'' luminescence signal in the presence of target DNA.[19-23] This kind of probe can cause negative results and is not suitable for analytical application because the quenching of the luminescence can be resulted from other quenchers. Thus, it is necessary to develop effective and sensitive "turn on" methods for detecting PML/RARα fusion gene with high sensitivity by using simple and inexpensive assays.

To construct a LRET probe with high detection sensitivity, the key procedure is to design a donor-acceptor pair in which the emission of the energy donor and the absorbance of energy acceptor matches well to allow an efficient LRET process to take place.[24, 25] Lanthanide-doped upconversion nanoparticles (UCNPs), which are capable of converting near-infrared excitation light into shorter wavelength light have been proven to exhibit attractive optical and chemical properties, such as large stokes shifts, low toxicity, and resistance to photo-bleaching.[26] In fact, these merits make UCNPs as an ideal candidate of the luminescence donor in the LRET-based bioassays.[27-30] The graphite based structures with a large conjugate plane and sp^2 electronic hybrid have exhibited highly efficient quenching ability to luminescence,[31-34] and thus can act as an ideal energy acceptor. Most importantly, it has been documented that ssDNA can be strongly attached on the surface of graphene oxide relying on the strong noncovalent π-π stacking interaction between nucleobases of ssDNA and sp^2 carbon atoms of graphene oxide.[35] These results attract our attention to construct the LRET nanoprobe based on UCNPs and graphene oxide as the donor-acceptor pair for sensitive detection of PML/RARα fusion gene.

Compared with two-dimensional graphene oxide with a relatively large conjugate plane, the size of zero-dimensional single-walled carbon nanohorns (SWCNHs) is more favorable for bioassays. SWCNHs can be seen as a curl irregular cylinder made by single layer of graphene with a conical cap (the cone angel is about 20°) at one end.[36-39] SWCNHs assembles to form three different types of spherical aggregates, which are called dahlia-like, bud-like, and seed-like types.[40,41] Since SWCNHs hold the similar sp^2 electronic structure and conjugate plane, it is reasonable to expect that they have the same luminescence quenching ability as graphene oxide. In this work, we report a sensitive LRET nanoplatform for detection of PML/RARα fusion gene (Scheme 1). Citrate-capped $NaYF_4$:20%Yb,2%Er@$NaYF_4$ (Cit-UCNPs) and seed-taped SWCNHs

were used as energy donor and energy acceptor, respectively, to form the donor-acceptor pair. A probe ssDNA (5'-NH$_2$-TCT CAA TGG CTG CCT CCC-3') was designed to combine UCNPs with SWCNHs to fabricate the nanoplatform. When being challenged with the target PML/RARα fusion gene sequences, the luminescence of UCNPs would be recovered due to the inhibition of the LRET process. Compared with other detection systems using down-converting fluorophores in which the excitation and emission spectra usually overlap there is no spectra overlap for those of UCNPs because the excitation wavelength of the UCNPs falls into NIR region (980nm), a few hundred nanometers away from the emission wavelength of the UCNPs. In addition, by using graphene oxide (GO) as energy accepter, a nanoplatform Cit-UCNPs–ssDNA-GO was also prepared for contrastive analysis. The SWCNHs were demonstrated as ideal energy acceptors because the nanometer size of the SWCNHs endowed them a larger interaction surface with UCNPs. To the best of our knowledge, this is the first time that UCNPs and SWCNHs were used as a donor-acceptor pair for detecting PML/RARα fusion gene sequences.

2. Results and discussion

The hydrophobic NaYF$_4$:20%Yb, 2%Er (UCNPs) and NaYF$_4$:Yb,Er@NaYF$_4$ (CS-UCNPs) were synthesized by solvent-thermal process, and the typical transmission electron microscopy (TEM) images of the as-synthesized nanoparticles were shown in Fig. 1. UCNPs and CS-UCNPs display uniform morphology and high quality with diameters of 28~30 nm and 33-35 nm, respectively (Fig. 1A and 1B). The citrate modified nanoparticles (Cit-UCNPs) remained uniform in water with almost unchanged particle sizes and shapes compared with CS-UCNPs (Fig. 1C). After combination with amine-functionalized ssDNA, the obtained Cit-UCNPs–ssDNA was still well dispersed in water and no aggregation could be observed (Fig. 1D). The Cit-UCNPs and Cit-UCNPs–ssDNA exhibited the strong green emission centered at 545 nm under the excitation at

980 nm (Fig. S1, ESI), which enabled them to act as ideal candidates for luminescence donor in the LRET-based bioassays. The TEM images of the energy acceptor, graphene oxide and single-walled carbon nanohorns, were shown in Fig. 1E and Fig. 1F, and the high magnification image of SWCNHs were shown in Fig. 1G and 1H, respectively. Graphene oxide has micrometer length and diameter while SWCNHs exhibit spherical aggregate morphology with the diameter of 30~40 nm for each sphere. The size distributions were further confirmed by dynamic light scattering (DLS) measurement. As shown in Fig. S2 (ESI), the average hydrodynamic size of UCNPs, CS-UCNPs, Cit-UCNPs and Cit-UCNPs–ssDNAs were 48.2 nm, 57.3 nm, 68.1nm and 78.8 nm, respectively. The SWCNHs and GO exhibited the hydrodynamic sizes of 68 nm and 122 nm in water, respectively. Compared with graphene oxide, the smaller size of SWCNHs might be more suitable for bioassays.

The XRD pattern of energy donor $NaYF_4$:20%Yb, 2%Er is shown in Fig. S3, and the diffraction lines can be ascribed to the hexagonal structure of $NaYF_4$ (JCPDS No.16-0334). The successful ligand exchange reaction of the UCNPs could be further confirmed by FT-IR spectra. As shown in Fig. S4A, the bands at 2908 cm^{-1} and 2844 cm^{-1} attributed to the asymmetric and symmetric stretching vibrations of methylene (CH_2) in long alkyl chain of OA, and the absorption band at around 1561 cm^{-1} assigned to the stretching vibration of carboxyl groups (–COOH), can be observed obviously in the spectrum of OA-UCNPs. After the ligand exchange process, the bands at 2908 cm^{-1} and 2844 cm^{-1} nearly disappear and the new band at 1618 cm^{-1} appears, which suggests the successful replacement of OA with citrate ligand on the surface of the nanoparticles. Furthermore, the absorption bands at around 1632 cm^{-1} of the Cit-UCNPs–ssDNA can be ascribed to the stretching vibrations of the (–CONH) bond. Both the FT-IR spectra of SWCNHs and GO were also obtained. As shown in Fig. S4B, in the curves of SWCNHs and GO, the peaks at 3440

cm^{-1} and 1640 cm^{-1} were attributed to the stretching vibrations of -OH and the bending vibration of C-OH, repectively. The peaks at 1380 cm^{-1}, 1140 cm^{-1} could be assigned to C-O-C and C-O stretching vibration respectively. In the spectrum of GO, the bands located at 1720 cm^{-1} were assigned to the stretching vibration of C=O. The presence of these hydroxyl groups further indicated that SWCNHs and GO exhibited good solubility in water. Fig. S5 showed the N_2 adsorption–desorption isotherms of SWCNHs and GO, the Brunauer–Emmett–Teller (BET) surface area of SWCNHs and GO were 43 m^2 g^{-1} and 64 m^2 g^{-1}, respectively. The Z-potential of the CS-UCNPs in cyclohexane was 53.2±0.43 mV, (Fig. S6, ESI). After the citrate modification, the obtained Cit-UCNPs exhibited a negative zeta potential of -20.5±0.21 mV, which was attributed to the carboxylate groups on the nanoparticle surface. As for Cit-UCNPs–ssDNA, after the attachment of ssDNA, the surface charge was changed into 9.5±0.39 mV. Therefore, these results further demonstrat the successful immobilization of Cit-UCNPs with the capture probe DNA.

Previous researches reported that the graphite based structures with a large conjugate plane and sp^2 electronic hybrid exhibited highly efficient quenching ability to luminescence. In this case, the designed ssDNA of Cit-UCNPs–ssDNA can be strongly attached on the surface of SWCNHs by the noncovalent π-π stacking interaction between nucleobases of ssDNA and sp^2 carbon atoms of SWCNHs. As a result, the luminescence of UCNPs would be quenched due to the efficient LRET process between Cit-UCNPs and SWCNHs. To investigate the energy transfer efficiency of the LRET process, different amounts of SWCNHs (0.1 mg/mL) were added into a fixed concentration of Cit-UCNPs–ssDNA (0.11 mg/mL). As shown in Fig. S7A, the upconversion luminescence of ssDNA-functionalized UCNPs was quenched gradually in the presence of increasing amounts of SWCNHs. The quenching efficiency reached 52% when 4.65 μg/mL SWCNHs was used and such a quenching efficiency of UCNPs luminescence revealed the super-quenching ability of SWCNHs. In

addition, the luminescence quenching effect of graphene oxide on UCNPs was also investigated (Fig. S7B), and the quenching efficiency only reached 31% when 4.65 μg/mL GO was added. It is reasonable to deduce that GO is a honeycomb-shaped sheet of carbon atoms at micron levels, while SWCNHs with nanometer length and diameter can offer a larger interaction surface with UCNPs.

At the presence of PML/RARα fusion gene (target DNA), the complementary base pairing reaction will happen between the target DNA and the probe ssDNA, and a stable, rigid double helix DNA structures will be formed. As a result, the energy transfer process between UCNPs and SWCNHs might be hampered. Based on this fact, the detection of PML/RARα fusion gene would be realized by determining the restoration of upconversion luminescence. As shown in Fig. 2A, an obvious increase of the upconversion luminescence intensity was observed after the addition of target DNA into the complex Cit-UCNPs-ssDNA-SWCNHs biosystem. As shown in Fig. 2B, the upconversion luminescence intensity increased linearly with the increase of the target DNA concentration from 0 to 43.5 nM. The limit of detection (LOD) was calculated to be 0.28 nM at a signal to noise of 3. Furthermore, the luminescence spectra of complex Cit-UCNPs–ssDNA-GO nanoplatform upon different concentrations of target DNA were investigated (Fig. S8A) and the similar results were obtained. It could be seen that the luminescence intensity displayed a good linear relationship towards the concentration of target DNA in the range from 0 to 35.1 nM, and the detection limit was calculated to be 0.56 nM (Fig. S8B). Due to the nanosize of SWCNHs, the Cit-UCNPs-ssDNA-SWCNHs biosystem had the higher detection sensitivity than Cit-UCNPs-ssDNA-GO.

To assess the specificity of the nanoplatform towards PML/RARα fusion gene, the spectra of the nanoplatform towards some species that may exist in biological samples, including non-complementary DNA (NC-DNA) and single-base mismatch DNA (SBM-DNA) were examined.

These DNA were added into the Cit-UCNPs–ssDNA-SWCNHs system individually instead of PML/RARα fusion gene under the same conditions. As shown in Fig. S9, upon the addition of SBM-DNA and NC-DNA the luminescence intensities of Cit-UCNPs–ssDNA-SWCNHs were nearly not changed, implying that these ssDNA possessed negligible interfering effect on PML/RARα fusion gene detection by Cit-UCNPs–ssDNA-SWCNHs. The similar results were also obtained from the luminescence spectra of Cit-UCNPs–ssDNA-GO nanoplatform upon addition of SBM-DNA (Fig. S10A) and NC-DNA (Fig. S10B). These results demonstrated the high specificity of the nanoplatform towards PML/RARα fusion gene.

In summary, a novel DNA nanoplatform based on luminescence resonance energy transfer from UCNPs to single-walled carbon nanohorns for PML/RARα fusion gene detection was prepared. The as-synthesized Cit-UCNPs-ssDNA-SWCNHs nanoplatform has the capability for PML/RARα fusion gene sensing in aqueous solution with a detection limit of 0.28 nM. The SWCNHs was demonstrated as an ideal energy acceptor than lamellar GO due to its smaller size. We expect that the adaptability of this strategy may be further developed for clinical applications in the future.

Acknowledgments

Reference

1.   R. E. Gallagher, *Blood*, 2002, **101**, 2521-2528.

2.   Z. X. Shen, Z. Z. Shi, J. Fang, B. W. Gu, J. M. Li, Y. M. Zhu, J. Y. Shi, P. Z. Zheng, H. Yan, Y. F. Liu, Y. Chen, Y. Shen, W. Wu, W. Tang, S. Waxman, H. De The, Z. Y. Wang, S. J. Chen and Z. Chen, *Proc. Natl. Acad. Sci. USA*, 2004, **101**, 5328-5335.

3.   R. Ohno, N. Asou and K. Ohnishi, *Leukemia*, 2003, **17**, 1454-1463.

4.   M. S. Tallman, J. W. Andersen, C. A. Schiffer, F. R. Appelbaum, J. H. Feusner, W. G. Woods, A. Ogden, H. Weinstein, L. Shepherd, C. Willman, C. D. Bloomfield, J. M. Rowe and P. H. Wiernik, *Blood*, 2002, **100**, 4298-4302.

5.   A. K. Burnett, D. Grimwade, E. Solomon, K. Wheatley and A. H. Goldstone, *Blood*, 1999, **93**, 4131-4143.

6.   Z. X. Chen, Y. Q. Xue, R. Zhang, R. F. Tao, X. M. Xia, C. Li, K. Wang, W. Y. Zu, X. Z. Yao and L. B. J., *Blood*, 1991, **78**, 1413-1419.

7.   N. Wei, J. H. Chen, J. Zhang, K. Wang, X. W. Xu, J. H. Lin, G. W. Li, X. H. Lin and Y. Z. Chen, *Talanta*, 2009, **78**, 1227-1234.

8.   M. S. Tallman, C. Nabhan, J. H. Feusner and J. M. Rowe, *Blood*, 2002, **99**, 759-767.

9.   A. Melnick and J. D. Licht, *Blood*, 1999, **93**, 3167-3215.

10. T. S. K. Wan, C. S. Chim, C. K. So, L. C. Chan and S. K. Ma, *Cancer. Gene. Cytogen.*, 1999, **111**, 39-143.

11. S. Dermime, F. Grignani, M. Clerici, C. Nervi, G. Sozzi, G. P. Talamo, E. Marchesi, F. Formelli, G. Parmiani, P. G. Pelicci and C. G. Passerini, *Blood*, 1993, **82**, 1573-1577

12. C. A. Tirado, V. Golembiewski-Ruiz, J. Horvatinovich, J. O. Moore, P. J. Buckley, T. T. Stenzel and B. K. Goodman, *Cancer. Genet. Cytogen.*, 2003, **145**, 31-37.

13.   S. J. Yoo, E. J. Seo, J. H. Lee, Y. H. Seo, P. W. Park and J. Y. Ahn, *Cancer. Genet. Cytogen.*, 2006, **167**, 168-171.

14.   G. Y. Lee, S. Christina, S. L. Tien, A. B. Ghafar, W. Hwang, L. C. Lim and T. H. Lim, *Cancer. Genet. Cytogen.*, 2005, **159**, 129-136.

15.   S. Abe, I. Ishikawa, H. Harigae and T. Sugawara, *Cancer. Genet. Cytogen.*, 2008, **184**, 44-47.

16.   J. Y. Han, K. E. Kim, K. H. Kim, J. I. Park and J. S. Kim, *Leuk. Res.*, 2007, **31**, 239-243.

17.   K. Wang, Z. Sun, M. Feng, A. Liu, S. Yang, Y. Chen and X. Lin, *Biosens. Bioelectron.* , 2011, **26**, 2870-2876.

18.   J. P. Yuan, W. W. Guo, X. R. Yang and E. K. Wang, *Anal. Chem.* , 2009, **81**, 362–368.

19.   G. X. Jiang, A. S. Susha, A. A. Lutich, F. D. Stefani, J. Feldmann and A. L. Rogach, *ACS Nano*, 2009, **3**, 4127–4131

20.   D. J. Zhou, L. M. Ying, X. Hong, E. A. Hall, C. Abell and D. Klenerman, *Langmuir*, 2008, **24**, 1659-1664.

21.   L. G. Xu, Y. Y. Zhu, W. Ma, H. Kuang, L. Q. Liu, L. B. Wang and C. L. Xu, *J. Phys. Chem. C* 2011, **115**, 16315-16321.

22.   A. A. Marti, S. Jockusch, N. Stevens, J. Ju and N. J. Turro, *Acc. Chem. Res.* , 2007, **40**, 402-409.

23.   Y. M. Miao, Z. F. Zhang, Y. Gong and G. Q. Yan, *Biosens. Bioelectron.* , 2014, **59**, 300-306.

24.   Q. Liu, Y. Sun, T. S. Yang, W. Feng, C. G. Li and F. Y. Li, *J. Am. Chem. Soc.* , 2011, **133**, 17122-17125.

25.   Y. M. Yang, F. Liu, X. G. Liu and B. G. Xing, *Nanoscale*, 2013, **5**, 231-238.

26.   L. Z. Zhao, J. J. Peng, Q. Huang, C. Y. Li, M. Chen, Y. Sun, Q. N. Lin, L. Y. Zhu and F. Y. Li,

Adv. Funct. Mater. , 2013, **24**, 363–371.

27.   M. N. Wang, X. J. An and J. Gao, *J. Lumin.* , 2013, **144**, 91-97.

28.   L. Y. Wang, R. X. Yan, Z. Y. Huo, L. Wang, J. H. Zeng, J. Bao, X. Wang, Q. Peng and Y. D.
        Li, *Angew. Chem. Int. Ed.* , 2005, **44**, 6054-6057.

29.   Y. J. Ding, H. Zhu, X. X. Zhang, J. G. Gao, E. S. Abdel-Halim, L. P. Jiang and J. J. Zhu,
        Nanoscale, 2014, **6**, 14792-14798.

30.   J. N. Liu, W. B. Bu, L. M. Pan and J. L. Shi, *Angew. Chem., Int. Ed.*, 2013, **52**, 4375-4379.

31.   C. H. Liu, Z. Wang, H. X. Jia and Z. P. Li, *Chem. Commun.* , 2011, **47**, 4661-4663.

32.   Y. Wang, L. Bao, Z. Liu and D. W. Pang, *Anal. Chem.* , 2011, **83**, 8130-8137.

33.   R. S. Swathi and K. L. Sebastian, *J. Chem. Phys.* , 2008, **129**, 054703.

34.   R. S. Swathi and K. L. Sebastian, *J. Chem. Phys.* , 2009, **130**, 086101.

35.   P. Alonso-Cristobal, P. Vilela, A. El-Sagheer, E. Lopez-Cabarcos, T. Brown, O. L. Muskens,
        J. Rubio-Retama and A. G. Kanaras, *ACS Appl. Mater. Interfaces*, 2015, **7**, 12422-12429.

36.   K. Pramoda, K. Moses, M. Ikram, K. Vasu, A. Govindaraj and C. N. R. Rao, *J. Clust. Sci.*,
        2013, **25**, 173-188.

37.   J. Li, Z. He, C. R. Guo, L. P. Wang and S. K. Xu, *J. Lumin.* , 2014, **145**, 74-80.

38.   N. Sano, T. Suzuki, K. Hirano, Y. Akita and H. Tamon, *Plasma Sources Sci.Technol.*, 2011,
        20, 034002.

39.   N. Sano, T. Suntornlohanakul, C. Poonjarernsilp, H. Tamon and T. Charinpanitkul, *Ind. Eng.*
        Chem. Res. , 2014, **53**, 4732-4738.

40.   T. Azami, D. Kasuya, T. Yoshitake, Y. Kubo, M. Yudasaka, T. Ichihashi and S. Iijima, Carbon,
        2007, 45, 1364-1367.

41.   S. Iijima, M. Yudasaka, R. Yamada, S. Bandow, K. Suenaga, F. Kokai and K. Takahashi,
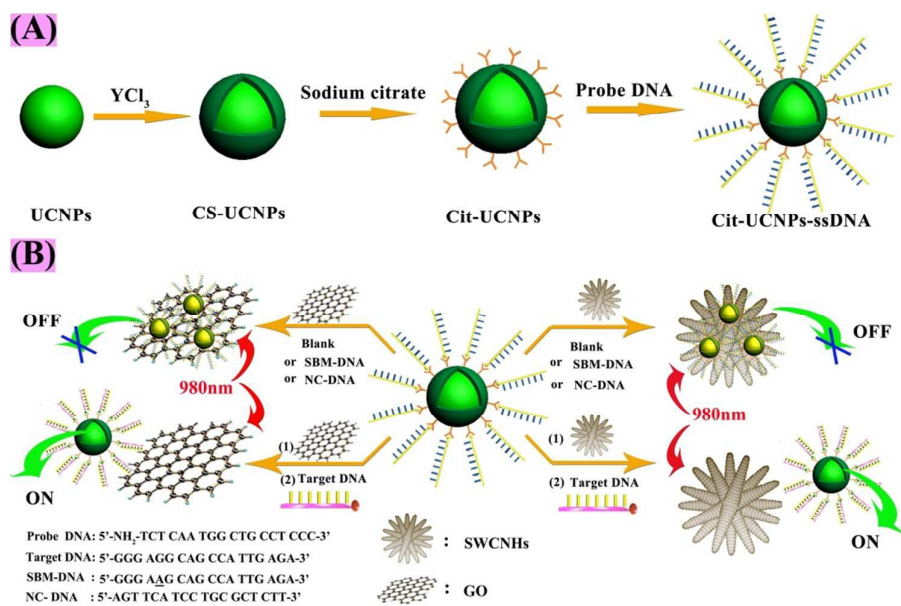
Chem. Phys. Lett. , 1999, 309, 165–170.

Figure Caption

Scheme 1. (A) Schematic illustration of the synthetic procedure for Cit-UCNPs-ssDNA; (B) Schematic illustration of the PML/RARα fusion gene nanoplatform on the basis of luminescence resonance energy transfer from Cit-UCNPs-ssDNA to single-walled carbon nanohorns or graphene oxide under excitation with 980 nm laser.

Figure 1. Typical TEM images of (A) OA-UCNPs, (B) CS-UCNPs, (C) Cit-UCNPs, (D) Cit-UCNPs, (E) graphene oxide, and (F) single-walled carbon nanohorns. (G) and (H) are the HRTEM images of single-walled carbon nanohorns.

Figure 2. (A) The luminescence spectra of multiplexed Cit-UCNPs–ssDNA-SWCNHs nanoplatform with various concentrations of target DNA (PML/RARα fusion gene). (B) Linear relationship between upconversion luminescence intensity recorded at 545 nm versus target DNA concentrations. Target DNA concentration in the range of 0 to 43.5 nM; the final concentration of Cit-UCNPs–ssDNA used was 0.11 mg/mL; SWCNHs: 4.65 μg/mL; λ_{ex}=980 nm. Experiments were performed in deionized water.

Probe DNA: 5'-NH₂-TCT CAA TGG CTG CCT CCC-3'
Target DNA: 5'-GGG AGG CAG CCA TTG AGA-3'
SBM-DNA : 5'-GGG AAG CAG CCA TTG AGA-3'
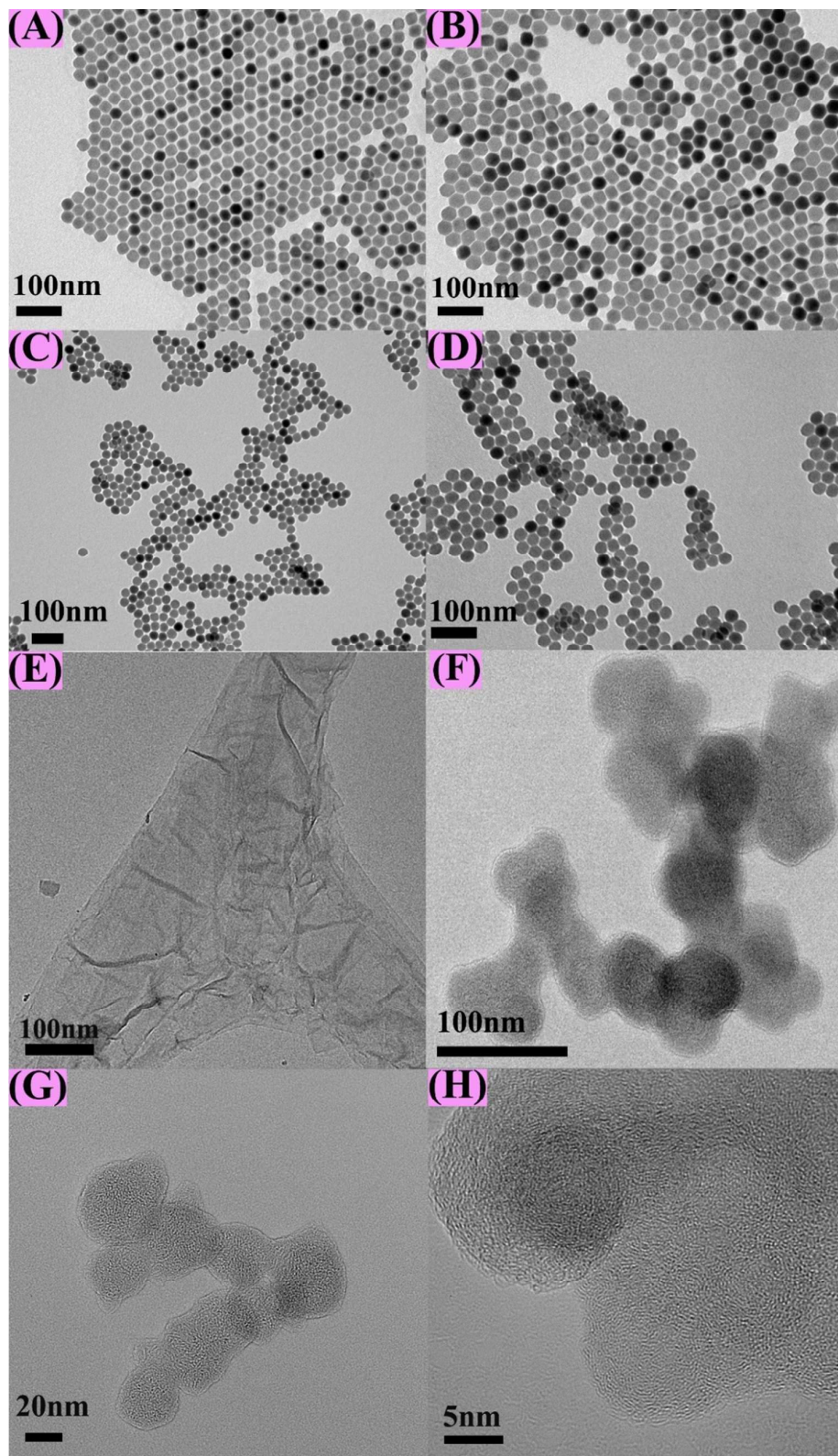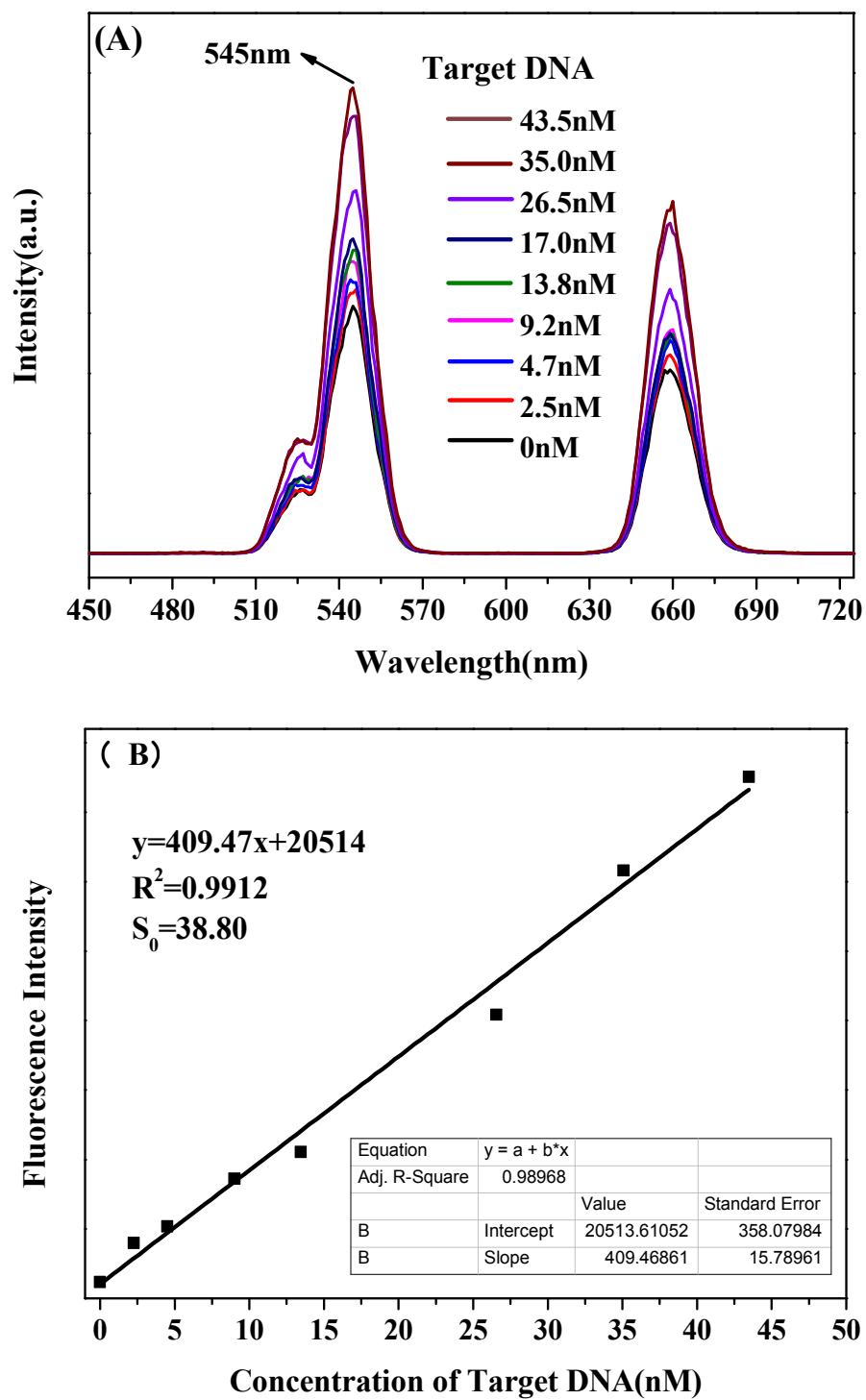NC- DNA : 5'-AGT TCA TCC TGC GCT CTT-3'

Scheme 1

Fig. 1

Fig. 2

New nanoplatforms based on upconversion nanoparticles and single-walled carbon nanohorns were prepared for sensitive detection of acute promyelocytic leukemia.